Multipolar dark matter freeze-out in an early matter-dominated universe

Debajit Bose,[1,*] Prolay Chanda,[2,†] Suvam Maharana,[2,‡] and Poulami Mondal[2,§]

[1]*Centre for High Energy Physics, Indian Institute of Science, C. V. Raman Avenue, Bengaluru 560012, India*
[2]*Department of Theoretical Physics, Tata Institute of Fundamental Research, Mumbai 400005, India*

(Received 20 July 2026; accepted 29 September 2026; published 30 October 2026)

The relic abundance of thermal dark matter depends not only on its particle interactions but also on the expansion history of the early Universe. We study the freeze-out of fermionic dark matter interacting with the Standard Model through higher-dimensional electromagnetic operators in an early matter-dominated cosmology. In particular, we consider magnetic-dipole, electric-dipole, anapole, and charge-radius interactions and compute the interaction strengths required to reproduce the observed dark matter relic abundance, accounting for the subsequent entropy injection from the decay of a long-lived heavy field. We compare the resulting parameter space with that obtained in the standard radiation-dominated freeze-out scenario and confront it with current constraints from direct-detection experiments and solar-neutrino searches. We find that the entropy dilution associated with an early matter-dominated epoch significantly reduces the interaction strength required to obtain the observed relic abundance, thereby opening regions of parameter space that are excluded within the conventional cosmological history.

DOI: 10.1103/44kt-wqn4

I. INTRODUCTION

The nature of particle dark matter (DM) remains one of the most intriguing puzzles in modern physics. In the absence of a clear detection thus far, the characterization of possible DM candidates is essentially governed by two fundamental elements, namely, the precise nature of the early Universe cosmology and the microscopic dynamics dictating the interactions of the DM candidates among themselves as well as with the Standard Model (SM) particles.

On the cosmological side, the Universe is generally understood to have been radiation-dominated during big bang nucleosynthesis (BBN) [1]. Owing to our limited knowledge of the pre-BBN era, a common assumption is, therefore, that radiation domination persisted from post-inflationary reheating until BBN. However, alternative thermal histories of the early Universe remain viable, since there is no direct evidence requiring the Universe to have been radiation dominated throughout the entire period between inflationary reheating and BBN. The possibility of such *nonstandard* cosmologies has elicited extensive studies of their attendant consequences, especially in the context of DM physics [2–17].

The weakly interacting massive particle (WIMP) paradigm has historically provided a compelling DM candidate, since stable particles with weak-scale masses and weak-strength interactions naturally produce the observed relic abundance via thermal freeze-out [18].While DM freeze-out calculations are typically performed under the assumption of radiation domination, freeze-out may instead have taken place during an era in which the dominant energy density redshifted differently from radiation, thereby affecting the DM freeze-out dynamics. DM freeze-out during an early matter-dominated era is one of such scenarios that has been studied in Ref. [19], following the original motivation of Ref. [2]. It assumes the presence of a heavy field that comes to dominate the energy density of the Universe, leads to an early period of matter domination, and subsequently decays into radiation prior to BBN, thereby injecting entropy into the thermal bath. An important consequence of an early matter-dominated era is that it allows for overproduction of DM at freeze-out, which gets diluted later due to the entropy injection. Equivalently, this allows for weaker annihilation cross sections, which have been shown to reopen viable parameter space for otherwise strongly constrained DM freeze-out models [19–22].

As for the particle identity of DM and its interactions with SM particles, there exist a plethora of possibilities, most notably within the WIMP paradigm [23–28]. What then serves to reduce the number of possibilities is the assumption of minimality. One such minimal, albeit

*Contact author: debajitbose550@gmail.com
†Contact author: prolay.chanda@tifr.res.in
‡Contact author: suvam.maharana_528@tifr.res.in
§Contact author: poulami.mondal@tifr.res.in

Published by the American Physical Society under the terms of the Creative Commons Attribution 4.0 International license. Further distribution of this work must maintain attribution to the author(s) and the published article's title, journal citation, and DOI. Funded by SCOAP³.

interesting, possibility is that DM interacts only electromagnetically with the SM sector. The scenario in which DM carries an electric charge is strongly disfavored by cosmological observations [29,30], astrophysical probes [31–33], and direct detection experiments [34]. Therefore, a well-motivated alternative is that DM is electrically neutral and yet interacts electromagnetically through higher-dimensional operators—the leading ones being characterized by electromagnetic multipole moments [35–43]. For a Dirac fermion DM, these comprise (up to dimension 6) the magnetic dipole moment, electric dipole moment, charge radius, and anapole operators. In the case of a Majorana fermion DM, the only possible electromagnetic couplings are furnished by the anapole operator and its higher moments [40,44].

However, previous studies of multipolar DM candidates have derived strong limits from direct detection [38,43,45–50], astrophysical and cosmological observations [48,51–53], and collider experiments [54–56]. When combined with the DM relic density requirement under the assumption of a radiation-dominated freeze-out scenario, these bounds leave the parameter space strongly constrained. In this work, our key goal is to consider the case of matter-dominated freeze-out as discussed in the previous paragraphs and explore whether an alternative early cosmology can help evade the existing experimental bounds on the parameter space.

This paper is structured as follows. In Sec. II, we discuss the matter-dominated freeze-out scenario and calculate the DM relic abundance after freeze-out and the subsequent entropy injection. In Sec. III, we mention several ways a neutral DM candidate can interact with the SM electromagnetically and derive the DM annihilation cross section to the SM for such models. In Sec. IV, we present the allowed parameter space and discuss how an early matter-dominated era relaxes the experimental constraints on the multipolar DM models considered in this work. We finally conclude in Sec. V.

II. MATTER-DOMINATED DARK MATTER FREEZE-OUT

In this section, we discuss the DM freeze-out mechanism in an early matter-dominated cosmology, originally proposed in Ref. [19]. We elaborate on the differences between the matter-dominated freeze-out from the conventional radiation-dominated freeze-out mechanism, for example, the change in the expansion history and the presence of a heavy field that results in early matter-dominated era. We present an analytic prescription for the Boltzmann analysis for calculating the freeze-out temperature and DM relic density.

A. General setup and dark matter relic abundance

Following the discussion of Ref. [19], we introduce a sufficiently long-lived heavy scalar ϕ that starts evolving as matter at a critical temperature $T_\star$ such that its energy density ρ_ϕ scales as a^{-3}, where a is the cosmological scale factor. Therefore, given ϕ is long lived enough, there will be a matter-dominated period in the early Universe. In the simplest scenario, ϕ decouples from the thermal bath so that ϕ starts behaving as matter at $T_\star \sim m_\phi$, where m_ϕ is the mass of the heavy scalar.[1] This early matter domination ends following the decay of the ϕ field and transitions to a radiation-dominated era. From here on, every quantity with subscript $\star$ is evaluated at $T = T_\star$.

The fraction of energy density contained in radiation at $T_\star$ can be defined as

$$r \equiv \left.\frac{\rho_R + \rho_\chi}{\rho_R + \rho_\chi + \rho_\phi}\right|_{T=T_*}, \tag{1}$$

where, ρ_χ and ρ_R are the energy density of the DM, χ, and the SM thermal bath, respectively.

When $T > T_\star$, both the DM and ϕ behave as radiation along with the SM thermal bath. The energy density of the radiationlike component is determined as $(\pi^2/30) g_R T^4$, where g_R is the internal degrees of freedom in radiation.

The Hubble parameter is determined by the total energy budget of the Universe,

$$H^2 = \frac{8\pi}{3M_{\rm Pl}^2}(\rho_R + \rho_\phi + \rho_\chi), \tag{2}$$

which, for practical purposes, we rewrite in the following form:

$$\frac{H^2}{H_\star^2} = \left[\frac{g_* r}{g_* + g_\chi}\left(\frac{a_\star}{a}\right)^4 + (1-r)\left(\frac{a_\star}{a}\right)^3 + \frac{g_\chi r}{g_* + g_\chi}\left(\frac{a_\star}{a}\right)^4\right]. \tag{3}$$

Here, the normalization factor is the Hubble parameter, $H_\star \equiv H(T_\star) \approx \sqrt{4\pi^3/45}\, g_*^{1/2}(T_\star) T_\star^2/M_{\rm Pl}$, because $g_* \gg g_\chi, g_\phi$, where, g_*, g_χ, and g_ϕ are the internal degrees of freedom of the SM, DM, and ϕ.

Assuming entropy conservation in the radiation bath prior to significant ϕ decay, the scale factor a and temperature T are related as

$$\left(\frac{a_\star}{a}\right) \simeq \left[\frac{g_*(T)}{g_*(T_\star)}\right]^{1/3} \frac{T}{T_\star}, \tag{4}$$

[1] In general, if ϕ is decoupled from the thermal bath, $T_\star$ represents the Standard Model temperature at which ϕ becomes matterlike. Also, ϕ could be a fermion or a vector boson instead of a scalar. Importantly, ϕ is assumed to have no coupling with the DM at the tree level.

allowing the Friedmann equation to be expressed explicitly in terms of T.

B. Modified Hubble expansion and freeze-out condition

The freeze-out condition is defined by equating the DM annihilation rate per DM particle $\Gamma_{\mathrm{ann},\chi}$, with the Hubble parameter

$$\Gamma_{\mathrm{ann},\chi} = H(T_{\mathrm{f}}), \tag{5}$$

such that at a thermal bath temperature T_{f} the DM particles cease to annihilate and their abundance freezes out.

Thus, the freeze-out conditions depend strongly on the expansion history of the Universe—namely, the standard radiation-dominated universe ($H \propto T^2$), early matter-dominated universe ($H \propto T^{3/2}$) [2,19], particle decay/heating ($H \propto T^4$) [3,57], kination ($H \propto T^3$) [58], etc.

We consider the simplest scenario of a purely matter-dominated Universe such that the decay of ϕ can be neglected when the DM freeze-out occurs. Apart from the different expansion rate in an early matter-dominated Universe, the entropy produced by the decay of ϕ dilutes the DM abundance produced at freeze-out, reducing the relic abundance by a factor ζ,

$$\Omega_{\mathrm{relic},\chi} = \zeta \Omega_{\mathrm{f},\chi}, \tag{6}$$

which we call as the entropy dilution factor.

We define the decay temperature T_Γ as the point when the ϕ decay width Γ_ϕ becomes comparable to the Hubble expansion rate $H(T_\Gamma)$. In the sudden decay approximation, the reheating temperature, T_{RH},[2] corresponding to ϕ is given as $T_{\mathrm{RH}} \simeq \sqrt{\Gamma_\phi M_{\mathrm{Pl}}}$, and the entropy dilution factor is given as [11]

$$\zeta \equiv \frac{s_{\mathrm{before}}}{s_{\mathrm{after}}} \simeq \left(\frac{T_\Gamma}{T_{\mathrm{RH}}}\right)^3, \tag{7}$$

where $s_{\mathrm{before}}(s_{\mathrm{after}})$ is the entropy density before (after) ϕ decay. Using Eqs. (4) and (7), we can derive the following form for T_Γ, relating T_{RH} and the dilution factor [20]

$$T_\Gamma \simeq \left(\frac{45}{4\pi^3 g_\star (1-r)} \frac{T_{\mathrm{RH}}^4}{T_\star}\right)^{1/3}. \tag{8}$$

C. Dark matter yield and relic density

In the initially radiation-dominated Universe, at a temperature $T_\star$, the ϕ field becomes nonrelativistic, and its energy density grows relative to radiation and eventually drives the Universe into matter domination. We denote by T_{MD} the temperature at which this transition occurs, defined as the point where the ϕ field contributes half of the total energy density. This temperature is related to $T_\star$ via [20,21]

$$T_{\mathrm{MD}} = \frac{1-r}{r}\left(\frac{g_*(T_\star)}{g_*(T_{\mathrm{MD}})}\right)^{1/3} T_\star. \tag{9}$$

In both matter- and radiation-dominated cosmologies, the Hubble parameter scales inversely with time t. It is therefore convenient to adopt the parametrization

$$H = \frac{\nu}{t}, \tag{10}$$

with $\nu = 2/3$ and $\nu = 1/2$ for matter and radiation domination, respectively.

The Boltzmann equation for the DM relic abundance Y_χ is

$$\frac{dY_\chi}{dt} = -\langle\sigma v\rangle s(T)(Y_\chi^2 - Y_{\chi,\mathrm{eq}}^2), \tag{11}$$

where $x = m_\chi/T$, $\langle\sigma v\rangle$ is thermally averaged annihilation cross section, $s(T)$ is the entropy density, and the equilibrium abundance for DM is [59]

$$Y_{\chi,\mathrm{eq}} = b x^{3/2} e^{-x}, \tag{12}$$

where $b = (45 g_\chi)/(4\sqrt{2}\pi^{7/2} g_{*S})$ and g_χ is the DM internal degrees of freedom (2 for complex scalar and 4 for Dirac fermion). The DM annihilation cross section can be expanded in a power series around $x = 0$,

$$\langle\sigma v\rangle = \sum_{n=0}^{\infty} \sigma_n x^{-n}. \tag{13}$$

The DM abundance equation can, then, be reorganized as

$$\frac{dY_\chi}{dx} = -\sum_n \lambda_n x^{-n-2} g_{\mathrm{eff}}^{1/2} (Y_\chi^2 - Y_{\chi,\mathrm{eq}}^2), \tag{14}$$

where the quantity λ_n contains the cross section and is defined as

$$\lambda_n = \nu \sqrt{\frac{4\pi}{45}} m_\chi M_{\mathrm{Pl}} \sigma_n, \tag{15}$$

with g_{eff} being the effective internal degrees of freedom given as

$$g_{\mathrm{eff}}^{1/2} \simeq g_\star^{1/2}(T_\star)\left(\frac{3T_\star(1-r)x}{4m_\chi} + r\right)\left(\frac{T_\star(1-r)x}{m_\chi} + r\right)^{-3/2}. \tag{16}$$

[2]Not to be confused with the inflationary reheating temperature.

As we show in Appendix A, an approximate analytic derivation of this differential equation provides the following form for the freeze-out abundance:

$$\Omega_{\rm relic}^{\rm MD} = \zeta \Omega_{\rm f}^{\rm MD},$$
$$\Omega_{\rm f}^{\rm MD} h^2 = \frac{10^9}{M_{\rm Pl}} \left(\sum_n \frac{\sqrt{g_*}(1-r)^{-1/2} x_\star^{1/2} \sigma_n \,\text{GeV}}{(n+3/2) x_{\rm f}^{n+3/2}} \right)^{-1}. \quad (17)$$

For reference, in the case of radiation-dominated freeze-out [60], the relic density is given as

$$\Omega_{\rm relic}^{\rm RD} h^2 = \Omega_{\rm f}^{\rm RD} h^2 \simeq \frac{10^9}{M_{\rm Pl}} \left(\sum_n \frac{\sqrt{g_*}\sigma_n \,\text{GeV}}{(n+1) x_{\rm f}^{n+1}} \right)^{-1}. \quad (18)$$

The freeze-out temperature for matter domination and radiation domination is given as

$$x_{\rm f}^{\rm MD} = \ln \left[\tilde{A} m_\chi^{3/2} T_\star^{-1/2} (1-r)^{-1/2} \sum_n (n+1) \sigma_n x_{\rm f}^{-n-1} \right],$$
$$x_{\rm f}^{\rm RD} = \ln \left[\tilde{A} m_\chi \sum_n (n+1) \sigma_n x_{\rm f}^{-n-1/2} \right], \quad (19)$$

where the prefactor is defined as

$$\tilde{A} = \frac{\sqrt{45} g_\chi}{\sqrt{32}\pi^3} g_\star^{-1/2} M_{\rm Pl}.$$

A detailed derivation of the above equations is given in Appendix A. We also discuss in Sec. IV B the validity of sudden decay of ϕ, an assumption that we made while deriving the DM relic density during matter domination.

D. Consistency conditions

The freeze-out analysis presented before relies on several assumptions, particularly regarding the hierarchy of cosmological energy scales and the ordering of the relevant processes in the early Universe. In this section, we outline the cosmological consistency requirements necessary for the validity of our treatment.

With the characteristic scales defined, the parameter space relevant for matter-dominated freeze-out is restricted by the following consistency conditions:

(i) DM freeze-out happens during the matter-dominated epoch, $T_{\rm f} < T_{\rm MD} \lesssim T_\star$.

(ii) The reheating resulting from ϕ decays must occur before BBN, such that $T_{\rm RH} > T_{\rm BBN} \sim 10$ MeV, where $T_{\rm BBN}$ is the characteristic BBN temperature [61].

(iii) Freeze-out must occur well before the decay of ϕ becomes important. We therefore require $T_{\rm f} \gg T_\Gamma, T_{\rm RH}$ so that the matter-dominated freeze-out treatment remains applicable. For a continuous decay of ϕ, entropy production during freeze-out may require a more careful treatment, as discussed in Sec. IV B.

(iv) Finally, DM must be nonrelativistic at freeze-out, $T_{\rm f} < m_\chi/3$ [18].

When these conditions are satisfied, DM freeze-out occurs in a purely matter-dominated background, and the analytical treatment developed in the previous section provides an accurate description of the relic abundance.

It is important to note, however, that the parameter space beyond this region is not necessarily excluded but instead requires a more careful analysis.

III. MULTIPOLE DARK MATTER: THEORETICAL RECIPE

In this section, we define the electromagnetic interactions of an electrically neutral DM candidate and delineate their implications for DM annihilation and scattering processes. As previously stated, such a DM species can have effective couplings with the photon through electromagnetic moments. Up to mass dimension 6, these electromagnetic interactions are most generally specified by the CP-even magnetic dipole moment (MDM), charge radius (CR) and anapole (AP) operators, and the CP-odd electric dipole moment (EDM) operator. Assuming a spin-1/2 fermion (χ) as the DM candidate, these operators are explicitly defined as

$$\mathcal{L}_{\rm MDM}^{(5)} = \frac{g}{\Lambda} \bar{\chi} \sigma^{\mu\nu} \chi F_{\mu\nu} \quad \text{(magnetic dipole)}$$
$$\mathcal{L}_{\rm EDM}^{(5)} = \frac{ig}{\Lambda} \bar{\chi} \sigma^{\mu\nu} \gamma^5 \chi F_{\mu\nu} \quad \text{(electric dipole)}$$
$$\mathcal{L}_{\rm CR}^{(6)} = \frac{g}{\Lambda^2} \bar{\chi} \gamma^\mu \chi \partial^\nu F_{\mu\nu} \quad \text{(charge radius)}$$
$$\mathcal{L}_{\rm AP}^{(6)} = \mathcal{C}_{\rm AP} \frac{g}{\Lambda^2} \bar{\chi} \gamma^\mu \gamma^5 \chi \partial^\nu F_{\mu\nu} \quad \text{(anapole)}, \quad (20)$$

with coefficients characterized by a dimensionless parameter g and a cutoff scale Λ.[3] Here, $F_{\mu\nu}$ is the electromagnetic field strength, and $\sigma^{\mu\nu} = (i/2)[\gamma^\mu, \gamma^\nu]$ denotes the spin tensor. Although the preceding list of operators is most generally allowed for a Dirac fermion, it must be noted that for a Majorana fermion the dipole moments and the charge radius operator vanish identically, leaving the anapole moment as the leading gauge-invariant coupling to the photon [40,44]. Accounting for this possibility, we include in $\mathcal{L}_{\rm AP}$ the prefactor $\mathcal{C}_{\rm AP} = 1(1/2)$ for Dirac (Majorana) fermions.

As the processes governing the DM phenomenology are annihilation (to SM particles) and scattering (off nucleons), it is perhaps instructive to get a qualitative idea of the

[3]Presumably, these operators are loop-induced moments generated by a heavy, charged, dark sector particle running in the loop with a characteristic scale $\sim\Lambda$.

possible effects of the aforementioned higher-dimensional operators on the nature of the corresponding cross sections. In particular, an estimate of the energy-momentum dependence of the said cross sections would be directly relevant in the discussions to follow regarding the DM's freeze-out dynamics as well as the constraints derived from direct detection experiments and indirect observations. To address these aspects systematically, we note that DM annihilations proceed either through an s-channel exchange of a photon or through a t-channel process mediated by the DM propagator itself. On the other hand, the DM-nucleon scattering, understandably, proceeds solely via a t-channel photon exchange. For brevity, we discuss the photon and DM mediated processes individually as follows.

Photon exchange: The $2 \to 2$ s-channel processes in this case are $\chi\bar{\chi} \to f\bar{f}, W^+W^-$, where f denotes the SM fermions. The t-channel exchange corresponds to the DM-nucleon scattering $\chi N \to \chi N$. The amplitudes of these processes can be written in a general current-current interaction form, namely,

$$\mathcal{M} = \frac{J^{\mu}_{\chi}(p_1, p_2; q) J_{\mu,\mathrm{SM}}(k_1, k_2; q)}{q^2}, \tag{21}$$

where the factor J^{μ}_{χ} specifies the dark sector current originating from the multipole operators and J^{μ}_{SM} denotes the contribution emanating from a purely SM current. The currents in general depend on the momenta of the DM and the visible sector particles, namely, (p_1, p_2) and (k_1, k_2), respectively. The variable q denotes the momentum exchange flowing through the photon propagator, which goes as $q^2 = s$ for s-channel annihilations and $q^2 = t$ for scatterings, where s and t are the usual Mandelstam variables. With the above definition in place, the following remarks are now in order:

(i) First, the derivatives in the operators have a contrasting, and in fact opposite, role to play in DM annihilations as compared to scattering processes. The mentioned processes being mediated by a photon, the derivative couplings simply translate to an additional dependence on the momentum exchange (q) via the photon propagator. Therefore, the net dependence of the dark sector currents on q can be readily factored out as

$$\begin{aligned} J_{\chi,\mu} &\propto (q_\rho \eta_{\mu\sigma}) \mathcal{J}^{\rho\sigma}_{\chi} \quad \text{(for dipoles)} \\ &\propto (q^2 \eta_{\mu\nu} - q_\mu q_\nu) \mathcal{J}^{\nu}_{\chi} \quad \text{(for AP and CR)} \end{aligned} \tag{22}$$

where $\mathcal{J}_{\chi}$'s encapsulate the spinorial pieces of the currents.

Clearly then, the explicit dependence on momentum transfer in the currents leads to an enhancement in the cross sections in the case of DM annihilations (when $q^2 = s$) and to a suppression in the case of a low-energy scattering off a nucleon (when $q^2 = t$). By comparing the Lorentz structure of the currents, we see that the annihilation cross section in the case of an anapole or charge radius DM is expected to receive a larger enhancement (by a factor of $s \sim 4m_\chi^2$) as compared to that for a dipole DM. By the same argument, then, the scattering cross section involving an AP or CR DM would be relatively more suppressed.

(ii) Apart from the dependence on the momentum exchange, the amplitudes also depend on the momenta of the incoming DM particle(s). The order at which the 3-momenta of the DM particles enter the amplitudes determines the nature of the annihilation cross sections vis à vis their dominant partial-wave behavior. The expected behavior can already be gleaned at the Lagrangian level, at least qualitatively, by looking at the transformation properties of the operators under parity. With the P-even operators (MDM and CR), the DM annihilation cross sections is understood to be dominantly s-wave in nature, whereas a p-wave nature is expected with an odd number of insertions of the P-odd ones (AP and EDM). This is most explicitly realized by reducing the spinor structure of the operators in the nonrelativistic (NR) limit and keeping terms to lowest order in the DM 3-momenta. For instance, for the specific case of an anapole DM which is a Dirac fermion annihilating to a pair of SM fermions (f), the amplitude in the center of mass frame in the NR limit reduces to

$$\begin{aligned} &[\bar{v}_\chi(p_2)\gamma^\mu\gamma^5 u_\chi(p_1)][\bar{u}_f(k_1)\gamma_\mu v_f(k_2)] \\ &\quad \overset{\mathrm{NR}}{\to} 2im_f[\xi^\dagger_2(\vec{p}_1 \times \vec{\sigma})_i \xi_1][\phi^\dagger_1 \sigma_i \phi_2] + \mathcal{O}(\vec{p}^3), \end{aligned} \tag{23}$$

where σ_i are the usual Pauli spin matrices and $\xi_{1,2}$ are the two-component Pauli spinors corresponding to $(u, v)_\chi$, respectively, and so are $\phi_{1,2}$ for the SM fermions. Being linear in $\vec{p}$ at the leading order, the NR amplitude clearly suggests a p-wave nature of the cross section associated with it. For reference, a complete list of the NR limits and the corresponding partial-wave behavior of the multipole operators is summarized in Table I. In the following subsection, we show explicitly the velocity dependence of thermally averaged cross section $\langle \sigma v_{\mathrm{rel}} \rangle$ for self-annihilation and scattering processes. We show, in particular, for the case of Anapole DM, that indeed $\langle \sigma v_{\mathrm{rel}} \rangle \propto v^2_{\mathrm{rel}}$.

DM exchange: The remaining channel for DM annihilation, *viz.*, $\chi\bar{\chi} \to \gamma\gamma$, is a t-channel process involving a DM propagator. Notably, the cross section for the process vanishes identically in the case of anapole and charge radius operators. For insertions of dipole operators, the general form of the amplitudes can be written as

TABLE I. Nonrelativistic structure of the multipole operators which appear in the amplitudes ($\mathcal{M}_{\rm ann}$) of the DM annihilation processes at the leading order in DM momenta. The partial-wave behavior of the corresponding cross sections is also listed for one insertion of the individual operators. Here, (ξ_1, ξ_2) are the two-component Pauli spinors corresponding to the Dirac spinors (u, v) of the DM field χ. The vector J denotes the SM electromagnetic current.

Interaction	Relativistic operator	P and C p roperties	NR structure in $\mathcal{M}_{\rm ann}$	Partial-wave scaling of $\langle\sigma v\rangle_{\rm ann}$
MDM	$\bar{\chi}\sigma^{\mu\nu}\chi F_{\mu\nu}$	P even, C even	$\xi_2^\dagger\vec{\sigma}\cdot\vec{E}\xi_1$	s-wave
EDM	$\bar{\chi}\sigma^{\mu\nu}\gamma^5\chi F_{\mu\nu}$	P odd, C even	$\xi_2^\dagger\vec{p}\cdot\vec{E}\xi_1$	p-wave
Anapole	$\bar{\chi}\gamma^\mu\gamma^5\chi J_\mu$	P odd, C odd	$\xi_2^\dagger(\vec{p}_1\times\vec{\sigma})\cdot\vec{J}\xi_1$	p-wave
Charge Radius	$\bar{\chi}\gamma^\mu\chi J_\mu$	P even, C even	$\xi_2^\dagger\vec{\sigma}\cdot\vec{J}\xi_1$	s-wave

$$\mathcal{M}_t \propto \frac{\bar{v}_\chi(p_2)\Gamma^{\mu\nu}(\not{p}_1 - \not{k}_1 + m_\chi)\Gamma^{\rho\sigma}u_\chi(p_1)}{t - m_\chi^2} k_{2\mu}k_{1\rho} \times \epsilon_\nu^*(k_2)\epsilon_\sigma^*(k_1) \tag{24}$$

$$\mathcal{M}_u \propto \frac{\bar{v}_\chi(p_2)\Gamma^{\mu\nu}(\not{p}_1 - \not{k}_2 + m_\chi)\Gamma^{\rho\sigma}u_\chi(p_1)}{u - m_\chi^2} k_{1\mu}k_{2\rho} \times \epsilon_\nu^*(k_1)\epsilon_\sigma^*(k_2) \tag{25}$$

for the t and u-channels, respectively. Here, $k_{1,2}$ are the photon momenta, and $\Gamma^{\mu\nu}$ acts as a placeholder for the gamma matrices present in the MDM and EDM operators.

Following the arguments made in the preceding segment, it is readily inferred that the cross section for the diphoton process will always be dominantly s-wave in nature. This is true even for an EDM DM due to the presence of two insertions of the P-odd operator in the amplitude. Also, since in the NR regime $t = u \approx -m_\chi^2$ and m_χ is the only mass scale present in the process, it is easy to estimate from dimensional analysis that the cross section would scale as $\sigma_{\gamma\gamma} \propto m_\chi^2/\Lambda^4$ for both MDM and EDM couplings.

Having illustrated the salient features of the various processes involving multipole DM operators, we present in the following subsection the expressions for the thermally averaged annihilation cross sections $\langle\sigma v_{\rm rel}\rangle_{\rm ann}$. We find that the explicit momentum dependence of $\langle\sigma v_{\rm rel}\rangle$ is in agreement with the preceding assertions. The detailed derivations of $\langle\sigma v_{\rm rel}\rangle$ are given in Appendix B. The expressions for the DM-nucleon scattering cross sections for these operators can be found in Refs. [50,62].

A. Expressions for annihilation cross sections

Here, we make a list of the thermally averaged annihilation cross section formulas in the NR limit as a power series expansion in the relative velocity $v_{\rm rel}$ of the incoming DM particles.[4] We invoke for the relevant processes only one multipole DM operator at a time[5] and categorize the expressions accordingly as follows:

1. For anapole

$$\begin{aligned}\langle\sigma v_{\rm rel}\rangle_{\chi\bar{\chi}\to f\bar{f}} &= \mathcal{C}_{\rm AP}^2\frac{2C_F\alpha g^2 m_\chi^2}{3\Lambda^4} \times\sqrt{1-\frac{m_f^2}{m_\chi^2}}\left(1+\frac{m_f^2}{2m_\chi^2}\right)\langle v_{\rm rel}^2\rangle,\\ \langle\sigma v_{\rm rel}\rangle_{\chi\bar{\chi}\to W^+W^-} &= \frac{2\alpha g^2 m_\chi^6}{3\Lambda^4 m_W^4}\langle v_{\rm rel}^2\rangle,\end{aligned} \tag{26}$$

2. For electric dipole moment

$$\begin{aligned}\langle\sigma v_{\rm rel}\rangle_{\chi\bar{\chi}\to f\bar{f}} &= \frac{C_F\alpha g^2}{3\Lambda^2}\sqrt{1-\frac{m_f^2}{m_\chi^2}}\left(1+\frac{m_f^2}{2m_\chi^2}\right)\langle v_{\rm rel}^2\rangle,\\ \langle\sigma v_{\rm rel}\rangle_{\chi\bar{\chi}\to W^+W^-} &= \frac{\alpha g^2 m_\chi^4}{3\Lambda^2 m_W^4}\langle v_{\rm rel}^2\rangle,\\ \langle\sigma v_{\rm rel}\rangle_{\chi\bar{\chi}\to\gamma\gamma} &= \frac{g^4 m_\chi^2}{\pi\Lambda^4}(8+5\langle v_{\rm rel}^2\rangle),\end{aligned} \tag{27}$$

[4]The thermally averaged relative velocity depends on the bath temperature T as $\langle v_{\rm rel}^2\rangle = 6x^{-1}$, where $x = m_\chi/T$.

[5]While this might seem an *ad hoc* assumption, it is quite possible to have DM models that dominantly induce only one of these operators in the IR. For example, the anapole operator is the only electromagnetic interaction possible for a Majorana DM as previously mentioned; for a Dirac fermion DM, the specific CP nature of the UV physics can lead to the generation of either the EDM or the MDM operator at the leading order. Naively, it is only in the case of the CR operator that one needs to assume a fine-tuned C and P-symmetric UV model so as to suppress the possible dimension-5 MDM operator in the IR relative to the dimension-6 CR operator. However, a discussion on the possible UV completions is beyond the scope of this work.

3. For magnetic dipole moment

$$\langle\sigma v_{\rm rel}\rangle_{\chi\chi\to f\bar{f}} = \frac{4C_F\alpha g^2}{\Lambda^2}\left(1-\frac{1}{24}\langle v_{\rm rel}^2\rangle\right),$$
$$\langle\sigma v_{\rm rel}\rangle_{\chi\chi\to W^+W^-} = \frac{4\alpha g^2 m_\chi^4}{\Lambda^2 m_W^4}\left(1+\frac{\langle v_{\rm rel}^2\rangle}{3}\right),$$
$$\langle\sigma v_{\rm rel}\rangle_{\chi\chi\to\gamma\gamma} = \frac{g^4 m_\chi^2}{\pi\Lambda^4}(8+5\langle v_{\rm rel}^2\rangle), \tag{28}$$

4. For charge-radius operator

$$\langle\sigma v_{\rm rel}\rangle_{\chi\chi\to f\bar{f}} = \frac{C_F\alpha g^2 m_\chi^2}{\Lambda^4}\left(4+\frac{7}{6}\langle v_{\rm rel}^2\rangle\right),$$
$$\langle\sigma v_{\rm rel}\rangle_{\chi\chi\to W^+W^-} = \frac{\alpha g^2 m_\chi^6}{\Lambda^4 m_W^4}\left(4+\frac{19}{6}\langle v_{\rm rel}^2\rangle\right) \tag{29}$$

where α is the electromagnetic fine-structure constant and C_F denotes the QCD color factor with a value $C_F = 3(1)$ for quarks (leptons). It is immediately apparent from the above expressions that the s-channel annihilations for the P-even operators are dominantly s-wave in nature while those involving the P-odd operators are p-wave suppressed, as was expected. The t-channel annihilation to $\gamma\gamma$ also, expectedly, exhibits an s-wave behavior for both MDM and EDM operators. Although the t-channel cross sections are $1/\Lambda^4$ suppressed, the additional m_χ^2 scaling of the same can render them comparable to the s-channel rates for large enough DM masses. For an EDM DM, the relative enhancement can be more pronounced due to the p-wave suppression of the s-channel processes. We further note that beyond the W-mass threshold, $m_\chi > m_W$, the W^+W^- channel dominates due to the apparent scaling of the cross sections as $\sigma \sim m_\chi^4, m_\chi^6$ obtained for dimension-5 and dimension-6 operators, respectively. However, these scalings are spurious in nature and should be understood as artifacts of the limited validity of the effective field theory (EFT) that we assume. We further elaborate on this point in the following section.

B. Note on EFT validity

As pointed out in the preceding section, the W^+W^- annihilation cross section through a photon exhibits a spurious energy growth, *viz.*, $\sigma \sim s^2, s^3$ for dimension-5 and dimension-6 operators, respectively. While a pathological energy growth is indeed expected on account of the nonrenormalizable nature of the multipole operators, a naive dimensional analysis suggests that the cross sections, at the worst, should scale as $\sigma \sim s^{D-5}$ for one insertion of an operator of mass dimension D. For instance, the process involving the anapole operator should have a scaling $\sigma \sim s$, i.e., similar to what is obtained for the $f\bar{f}$ annihilation. This implies that the enhanced energy growth obtained in the computations must be unphysical. The regime $m_\chi > m_W$, therefore, warrants caution since a naive inclusion of the W^+W^- channel can result in misleading identifications of viable regions in the dark sector parameter space.[6]

The bad high-energy behavior can be simply attributed to the fact that the inclusion of the W bosons as physical degrees of freedom breaks the manifest gauge invariance of the theory since the operators in Eq. (20) are written in terms of the electromagnetic field strength $F_{\mu\nu}$. Thus, the EFT description employed in Eq. (20) should be understood as the low-energy limit of a fully gauge-invariant theory defined above the electroweak (EW) symmetry breaking scale. In the unbroken phase, the multipole interactions are minimally expressed in terms of the hypercharge field strength $B_{\mu\nu}$, ensuring invariance under the full $SU(2)_L \times U(1)_Y$ gauge symmetry. After EW symmetry breaking, these induce couplings of the DM to both the photon and the Z boson. Understandably, then, DM annihilation to W^+W^- must necessarily include the Z mediated channel as well in order to restore gauge invariance in the computations. This indeed gets rid of the spurious energy scalings as shown in Refs. [64,65].

For $m_\chi > m_W$, a gauge-invariant treatment also opens the $\chi\bar{\chi} \to Zh$ channel, and, therefore, a more comprehensive analysis may require DM operators involving the SM Higgs as well.[7] Pursuing this, however, is beyond the scope of the present work, and for the sake of simplicity, we restrict our analysis to the regime $m_\chi < m_W$ where the operators defined in Eq. (20) provide a sufficient and well-behaved description of the target phenomenology.

In summary, the point of this discussion is to draw the readers' attention to the fact that the validity of the assumed EFT is not merely defined by the violation of perturbative unitarity near the UV cutoff scale Λ but also by the breakdown of gauge invariance beyond the EW scale.

IV. MULTIPOLE DARK MATTER: PHENOMENOLOGY, RESULTS, AND DISCUSSIONS

In the following, we first discuss the experimental constraints (direct detection and IceCube observations) employed in our analysis. We then consider a spin-1/2 fermionic DM candidate and study one effective operator at a time (i.e., setting the coefficients of all other operators to zero). For each operator, we present the DM relic density contours obtained for both the matter-dominated and

[6]This can be gleaned, e.g., from Ref. [63], which includes the W^+W^- annihilation channel mediated by a photon and retains the spurious divergence in the DM analysis.

[7]For example, if the multipole moments are generated by a (hypercharged) heavy scalar field, it will in general couple to the SM Higgs as well.

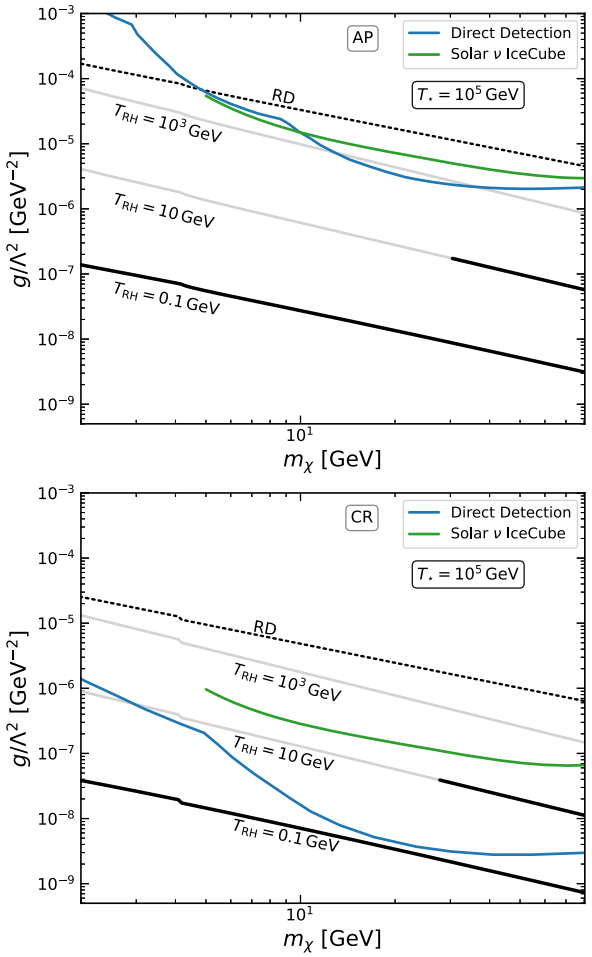


FIG. 1. Dimension-6 operators: relic density contours in the $(m_\chi, g/\Lambda^2)$ plane for the anapole interaction (top panel) and charge radius interaction (bottom panel), obtained by requiring the observed DM relic abundance, $\Omega_\chi h^2 = 0.12$, in the standard radiation-dominated (RD) cosmology and an early matter-dominated (MD) cosmology with varying reheating temperature $T_{\rm RH}$, and $r = 0.99$. Current constraints from direct detection and solar neutrino searches are also shown. Along the MD relic density contours, the solid black segments correspond to $T_f > T_{\rm EV}$ [Eq. (35)], while the gray segments correspond to $T_f < T_{\rm EV}$, where the freeze-out calculation requires a more careful treatment due to the significant decay of the matter field.

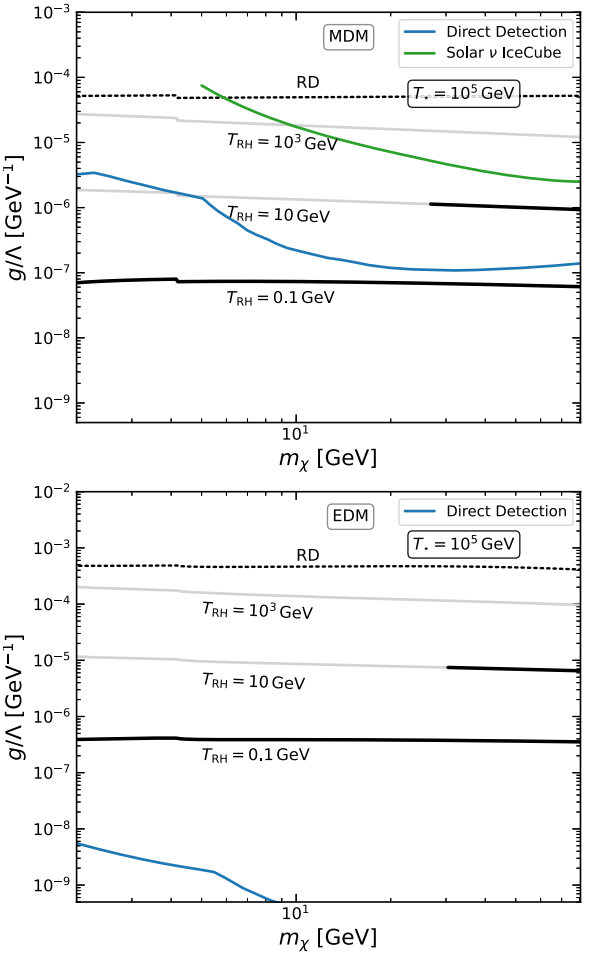


FIG. 2. Dimension-5 operators. relic density contours in the $(m_\chi, g/\Lambda)$ plane for the magnetic dipole interaction (top panel) and electric dipole interaction (bottom panel) operators, together with the corresponding constraints from direct detection constraints and solar neutrino searches. The contour definitions and color codings are the same as in Fig. 1.

radiation-dominated freeze-out and subsequently examine the viability of the corresponding parameter space in light of the current direct detection constraints.

A. Experimental constraints

1. Direct detection limits

For the direct detection limits, we extract the exclusion bounds for the anapole, dipole, and charge radius operators from Refs. [49,66,67]. Across the considered DM mass range, the leading bounds come from the electron recoil, Migdal, and nuclear recoil searches—PandaX-4T electron recoil limits [67] dominate at the lowest masses, the DarkSide-50 Migdal limit [49] dominates at the GeV scale, followed by the PandaX-4T nuclear recoil limits [66], after which the LUX-ZEPLIN (LZ) nuclear recoil limits [49] provide the strongest constraints. The LZ limits are determined up to 10^3 GeV in Ref. [49] utilizing WimPyDD [68]. For larger DM masses, the limits from different direct detection experiments are presented in Ref. [50]. The combined direct detection exclusion limits considered in our analysis are shown as the blue curve for each operators in Figs. 1 and 2.

2. Solar DM capture and GeV neutrinos

Another compelling direction to look for DM signatures is via the capture of DM particles inside celestial bodies due to DM scattering with nuclei and their annihilation into SM states, which would eventually give rise to neutrinos. These neutrinos can propagate through the stellar interior, escape

the celestial body, and eventually reach the terrestrial detectors [48,69–79]. Null observations of GeV neutrinos from the Sun can put limits on the DM couplings. In this work, we extract the limits on the anapole and dipole operators from Ref. [48]. For the charge radius operator, we derive the limit, and a brief discussion follows.

The capture rate of DM particles inside the Sun is given by [48,80,81]

$$C_\odot = \sum_k \left(\frac{\rho_0}{m_\chi}\right) \int_0^{R_\odot} 4\pi r^2 dr \times \int_0^{u_{\rm esc}} du_\chi \left(\frac{f_{v_\odot}(u_\chi)}{u_\chi}\right) w(r)\Omega_k^-(w), \quad (30)$$

where ρ_0 and u_χ are the local DM density and ambient DM velocity, respectively. The velocity distribution profile in the rest frame of the Sun, $f_{v_\odot}(u_\chi)$, is assumed to follow a Maxwell-Boltzmann distribution.[8] In Eq. (30), the velocity $w(r)$ denotes the DM velocity at a distance r from the center of the Sun, and the summation over k runs over the different nuclei inside the Sun. The term $\Omega_k^-(w)$ encapsulates the capture probability of a DM particle with velocity $w(r)$ interacting with the kth nucleus and is given by [51]

$$\Omega_k^-(w) = n_k(r) w(r) \int_{\frac{m_\chi u_\chi^2}{2}}^{\frac{m_\chi w(r)^2 \zeta_k}{2\zeta_{k,+}^2}} dE_{\rm nr} \frac{d\sigma_k}{dE_{\rm nr}}, \quad (31)$$

where n_k and m_k are the density and mass of the kth nucleus inside the Sun, with $\zeta = (m_\chi/m_k)$ and $\zeta_{k,+} = (\zeta_k + 1)/2$. The solar profile is extracted from Ref. [83]. The differential recoil rate for the charge radius operator is given by [50,62]

$$\left(\frac{d\sigma_k}{dE_{\rm nr}}\right)_{\rm CR} = \frac{2g^2\alpha}{\Lambda^4} \frac{Z_k^2 m_k}{u_\chi^2} F^2(E_{\rm nr}), \quad (32)$$

where Z_k is the atomic number of the kth nucleus and $F(E_{\rm ER})$ is the nuclear form factor, assumed to be the Helm form factor [84]. For the DM mass $m_\chi > 5$ GeV, evaporation is negligible [85,86], and the number of DM particles inside the Sun is dictated by capture and annihilation. Under the equilibrium condition, the annihilation rate can be related to the capture rate as $\Gamma_{\rm ann} = C_\odot/2$. The annihilation of DM particles inside the Sun can produce secondary neutrinos, and the differential neutrino flux reaching the Earth can be written as

$$E_\nu^2 \frac{d\Phi_\nu}{dE_\nu} = \frac{\Gamma_{\rm ann}}{4\pi D_\odot^2} \times \left(E_\nu^2 \frac{dN_\nu}{dE_\nu}\right), \quad (33)$$

where $D_\odot$ is the distance between the Sun and the Earth and dN_ν/dE_ν is the differential neutrino spectrum within the solar environment, generated using χAROν [87] for each of the SM final states and then summed over with the appropriate branching ratios. The neutrinos produced at the center of the Sun propagate through the solar interior, vacuum, the Earth, and its atmosphere, which is computed using NUSQUIDS [88], including neutrino oscillation, scattering, and tau regeneration.

After calculating the differential flux from Eq. (33), we compute the differential event rate following Refs. [48,73]. In Ref. [69], IceCube and DeepCore published three years of data on muon tracklike events as a function of the solar opening angle. Using the expected DM-induced neutrino flux from the solar direction together with the observed data, we perform a χ^2 analysis to determine the limits on the DM couplings at the 95% confidence level. Later, the IceCube Collaboration also analyzed 6.75 years of DeepCore data from the solar direction and provided upper limits on the DM annihilation rate for different SM final states [72]. We have recast those bounds in our scenario using the appropriate branching ratios and found that the $\tau^+\tau^-$ channel provides the most stringent bounds. The envelope of the bounds obtained above is calculated for the charge radius operator and is shown as the green curve in Fig. 1. For the anapole and magnetic dipole operators, the limits are shown in Figs. 1 and 2, respectively. For the electric dipole operator, the annihilation rate into fermions is suppressed, making the limits much weaker than those from direct detection. Therefore, we do not show them in this work.

B. DM freeze-out phenomenology and results

In this section, we determine the coupling strength required to reproduce the observed DM relic density within this alternative cosmological framework, and we assess the resulting parameter space in light of complementary constraints. Having set the stage in Sec. II by describing the freeze-out mechanism during a radiation-dominated as well as a matter-dominated era, we use the DM self-annihilation cross sections derived in Sec. III A and construct contours in the DM mass-coupling plane which satisfy the present day DM relic density [89]. We superimpose the experimental constraints over the relic contours to identify the allowed parameter space and, thereby, illustrate the viability of the aforementioned multipole DM models.

We show that the parameter space obtained under the standard radiation-dominated freeze-out is already highly constrained for electromagnetic multipole DM, in agreement with previous studies [48,49]. In contrast, we find that an early matter-dominated epoch substantially enlarges the viable parameter space through entropy dilution, allowing considerably weaker couplings while reproducing the observed relic abundance, which is the key result of our work. Among the four operators considered here, the

[8]The deviation from this distribution and its impact on the capture rate are discussed in Ref. [82].

electric dipole interaction remains strongly constrained even in the presence of an early matter-dominated era.

Using the analytic expressions in Eqs. (17)–(19), we determine the couplings required to reproduce the observed DM relic abundance for each electromagnetic multipole operator. The resulting relic density contours for the anapole, charge radius, electric dipole, and magnetic dipole interactions are shown in Figs. 1 and 2, together with the envelopes of the current direct detection and IceCube constraints from Sun. Throughout this analysis, we fix $T_\star = 10^5$ GeV, $r = 0.99$, and consider three representative reheating temperatures, $T_{\rm RH} = 0.1$, 10, and 10^3 GeV, characterizing the different amounts of entropy dilution while remaining safely above the BBN temperature.

As expected, the interaction strength required to obtain the observed relic abundance decreases as the reheating temperature is lowered. This effect can be understood directly from Eqs. (7) and (8) as the DM abundance dilution by entropy injection is correlated with the reheat temperature. Note that the matter-dominated freeze-out depends on an extra energy scale $T_\star$ and, therefore, has a different relation to m_χ compared to the radiation-dominated freeze-out as can be seen from Eqs. (17)–(19). This results in the apparent morphological difference between the corresponding relic contours.

The morphology of the relic density contours can be understood by dividing the parameter space into two physically distinct regimes. The first corresponds to the region where annihilation is dominated by fermionic final states for DM mass $m_\chi < m_W$. For the dimension-6 anapole and charge radius operators, the only relevant channel in this region is $\chi\bar{\chi} \to f\bar{f}$, since these operators do not induce the $\chi\bar{\chi} \to \gamma\gamma$ final state at leading order. Consequently, the corresponding relic density contours vary smoothly below the m_W threshold.

The second regime also lies below the m_W threshold but is specific to the magnetic and electric dipole operators, which receive contributions from both $\chi\bar{\chi} \to f\bar{f}$ and $\chi\bar{\chi} \to \gamma\gamma$. The fermionic contribution scales as $\langle\sigma v\rangle_{\chi\bar{\chi}\to f\bar{f}} \propto (g/\Lambda)^2$, whereas the diphoton channel scales as $\langle\sigma v\rangle_{\chi\bar{\chi}\to\gamma\gamma} \propto (g/\Lambda)^4 m_\chi^2$. At low reheating temperatures, the entropy dilution allows the observed relic abundance to be reproduced with substantially smaller effective couplings. The diphoton contribution is, therefore, suppressed relative to the fermionic channel which dominates the total annihilation cross section. This explains why the $T_{\rm RH} = 0.1$ GeV contours for the magnetic and electric dipole operators remain nearly flat for $m_\chi \ll m_W$. As the reheating temperature increases, the larger coupling required to obtain the correct relic abundance enhances the relative importance of the diphoton channel, producing the mild upward curvature observed below the electroweak threshold.

The phenomenological implications differ substantially among the four electromagnetic operators. For the anapole interaction, the relic density contours corresponding to $T_{\rm RH} = 10$ GeV and 0.1 GeV remain compatible with current direct detection and IceCube constraints over a substantial range of DM masses. For the magnetic dipole interaction and charge radius interaction, only the $T_{\rm RH} = 0.1$ GeV contour survives the existing limits, whereas the contours corresponding to larger reheating temperatures are excluded. In contrast, the electric dipole interaction is considerably more constrained, with almost the entire parameter space explored in this work being excluded irrespective of the cosmological history.

The stronger direct detection sensitivity of the electric dipole operator originates from its nonrelativistic interaction with the target nuclei. Unlike the magnetic dipole operator, the electric dipole interaction generates a coherent spin-independent contribution in addition to spin-dependent interactions [90], resulting in substantially stronger direct detection limits. Similar considerations apply to the charge radius operator, whose coherent interaction with nuclei also leads to stringent constraints from direct detection and GeV scale neutrino measurements from Sun at IceCube. Nevertheless, the entropy dilution associated with an early matter-dominated epoch enlarges the phenomenologically viable parameter space relative to the standard radiation-dominated freeze-out scenario.

The DM relic abundance calculation presented in Sec. II C assumes entropy conservation until when ϕ decays instantaneously at a time $\sim\Gamma_\phi^{-1}$. However, a more natural expectation is that ϕ decays through an exponential law [57]. In that case, while solving the Boltzmann equation, the entropy injection in the thermal bath will be non-negligible and, therefore, the freeze-out calculation should be carried out in the line of Giudice-Kolb-Riotto [3,91].

Thus, the total radiation energy density is the old radiation in the thermal bath plus the new radiation $\rho_{R,\rm Decay}$ produced by ϕ decay,

$$\rho_{R,\rm tot} = \rho_{R,\star}\left(\frac{a_\star}{a}\right)^4 + \rho_{R,\rm Decay}. \tag{34}$$

Scherrer and Turner [57] pointed out that entropy of the bath remains nearly unchanged until the new radiation becomes comparable to the old radiation. The entropy violation time frame can be derived by equating the first and second term of Eq. (34), and, as shown in Ref. [20], the temperature corresponding to the entropy violation is given as

$$T_{\rm EV} = T_\star\left(1 + \frac{r}{1-r}\frac{v}{\tau_\star}\right)^{(1-v)/v}, \tag{35}$$

where v is defined as

$$v = \frac{2}{3}(1+w)^{-1} + 1, \tag{36}$$

with w being the cosmological equation of state parameter relating pressure p and energy density ρ as $p = w\rho$. The dimensionless quantity $\tau = \Gamma_\phi t$.

For a continuous decay of ϕ, the entropy of the radiation bath remains approximately conserved for $T_{\rm f} > T_{\rm EV}$. For $T_{\rm f} \lesssim T_{\rm EV}$, radiation produced by the decay of ϕ becomes important, and the evolution enters the decay-dominated regime, where $T \propto a^{-3/8}$ [3]. The condition $T_f > T_\Gamma$ identifies freeze-out before the instantaneous decay event in our sudden-decay approximation. Continuous decay introduces a distinct scale, $T_{\rm EV}$, at which the decay-induced radiation becomes comparable to the preexisting bath. In Figs. 1 and 2, we use $T_{\rm EV}$ as the consistency condition, as this is stronger by an order of magnitude[9] compared to T_Γ.

We also note that, while the assumption of the electromagnetic-only DM couplings is consistent in its own accord as an EFT description below the EW scale, it disregards the possible effects of invoking Z-boson couplings for sub-EW scale DM masses. As shown in Ref. [64], these effects include the opening of the DM annihilation channel to $\nu\bar{\nu}$ and the resonance enhancement of the individual annihilation cross sections around the Z-pole. Thus, in connection to the relic-density calculations, this will invariably result in a dip in the associated contours in the coupling-vs-m_χ plane, a feature missing in our results in Figs. 1 and 2. While these deviations are quantitatively significant, their qualitative effect is simply identified as that it weakens the experimental and observational bounds on the parameter space around the resonance region, *viz.*, $m_\chi \sim m_Z/2$. Therefore, the expected changes will not invalidate any of our qualitative conclusions made within the purview of this work, which was to show how a nonstandard cosmological history can evade existing constraints on electromagnetically interacting DM. On the other hand, the aforementioned enhancement in the annihilation cross sections may also affect the indirect detection limits, namely, those derived from annihilations in galactic halos as well as from signals due to possible DM capture within celestial bodies. For the former, Ref. [64] (which assumes hypercharge couplings) finds that the bounds are typically weaker than those from direct detection; although they may probe parts of the radiation-dominated relic-density contours, they are not expected to exclude the lower-coupling contours for the matter-dominated scenarios. A similar conclusion holds true for the latter as well. This can be inferred by comparing the limits derived in this work using IceCube observations of solar neutrinos with those from a recent study [92] which has extended such capture-based probes to Earth, Jupiter, and white dwarfs.

[9]For example, with $T_{\rm RH} = 10$ GeV, $T_\star = 10^5$ GeV, and $r = 0.99$, we estimate $T_\Gamma \simeq 0.3$ GeV and $T_{\rm EV} \simeq 2.6$ GeV.

V. CONCLUSIONS

Electromagnetic multipole interactions provide a natural and minimal framework for an electrically neutral DM to couple to photons. In this work, we have shown that such interactions, although strongly constrained in the standard radiation-dominated freeze-out scenario, can remain phenomenologically viable in the presence of an early matter-dominated epoch. We have considered four multipole operators up to dimension 6, *viz.*, the magnetic dipole moment, electric dipole moment, anapole, and charge-radius operators. For each case, we have determined the coupling required to reproduce the observed DM relic abundance in both radiation- and matter-dominated cosmologies and confronted the resulting parameter space with current direct detection and IceCube solar neutrino constraints.

A generic feature of freeze-out during an early matter-dominated epoch is the entropy injection associated with the decay of the heavy matter field, ϕ. The resulting dilution of the DM abundance reduces the interaction strength required to reproduce the observed relic density compared with the standard radiation-dominated scenario. Consequently, regions of parameter space that are strongly constrained, or even excluded, by direct detection experiments and IceCube observations of neutrinos from the Sun in the conventional cosmological picture become viable in a nonstandard early cosmological history, which constitutes the key finding of this work. This effect is most pronounced for the anapole interaction, while the electric dipole operator remains strongly constrained over nearly the entire parameter space considered here. We have also identified the region where DM freeze-out occurs after the onset of significant decay of the heavy field. This region is not excluded but instead indicates where the simple freeze-out treatment adopted here should be refined by consistently incorporating heavy-field decay and entropy production during freeze-out. Such refinements are not expected to alter the main conclusions of this work.

Several directions remain to be explored. For DM masses above the electroweak scale, additional annihilation channels become relevant. Although the inclusion of these channels would be an improvement, a more comprehensive treatment ultimately requires a complete gauge-invariant operator basis including DM-Higgs interactions [93]. We defer a dedicated investigation for the heavy-mass regime to a future work, where we address these aspects in detail for freeze-out as well as for the freeze-in production during the decay-dominated phase.

Our results highlight that nonstandard cosmological histories can qualitatively alter the phenomenology of electromagnetic multipole DM, reopening regions of parameter space that appear excluded under the conventional radiation-dominated freeze-out paradigm.

Note Added. Recently, Ref. [94] appeared on the arXiv, presenting a related study of dipole DM models in the context of nonstandard cosmology. However, our work complements the authors' analysis by considering all possible electromagnetic operators for neutral DM up to dimension 6. Moreover, we point out the possible concerns and issues regarding the complete gauge invariance and EFT validity for DM masses beyond the EW scale, in contrast to the aforementioned paper.

ACKNOWLEDGMENTS

We sincerely thank Subhadip Bouri, Basudeb Dasgupta, Amol Dighe, Biprajit Mondal, Rohan Pramanick, and Akash Kumar Saha for their helpful discussions and insightful suggestions. We are indebted to Debajyoti Choudhury, Ranjan Laha, and James A. Unwin for useful discussions and for their valuable comments on the manuscript. D. B. acknowledges the Council of Scientific and Industrial Research (CSIR), Government of India, for supporting his research under the Research Associateship program through Grant No. 09/0079(24106)/2025-EMR-I. P. C., S. M. and P. M. are supported by the Department of Atomic Energy, Government of India, under Project Identification Number RTI-4012.

DATA AVAILABILITY

There are no publicly available research data or software supporting this manuscript. Requests for further information or data should be sent to the authors.

APPENDIX A: SOLUTION OF THE BOLTZMANN EQUATION

We start by defining a quantity Δ_χ, which is a measure of departure from the equilibrium abundance

$$\Delta_\chi = Y_\chi - Y_{\chi,\mathrm{eq}}; \tag{A1}$$

the Boltzmann equation in Eq. (14) can be rewritten as

$$\frac{d\Delta_\chi}{dx} = -\frac{dY_{\chi,\mathrm{eq}}}{dx} - \sum_n \lambda_n x^{-n-2} g_{\mathrm{eff}}^{1/2} (\Delta_\chi^2 + 2\Delta_\chi Y_{\chi,\mathrm{eq}}). \tag{A2}$$

At sufficiently late times, well after freeze-out ($x \gg x_f$), the temperature becomes low enough that Y_χ no longer follows its equilibrium value. In this regime, the abundance Y_χ becomes comparable to Δ_χ, since $Y_{\chi,\mathrm{eq}}$ is exponentially suppressed. Consequently, terms in Eq. (A2) involving $dY_{\chi,\mathrm{eq}}/dx$ and $Y_{\chi,\mathrm{eq}}$ can be neglected, and the evolution equation simplifies to

$$\frac{d\Delta_\chi}{dx} \simeq -\sum_n \lambda_n g_{\mathrm{eff}}^{1/2} x^{-n-2} \Delta_\chi^2. \tag{A3}$$

Integrating this expression over the interval $[x_f, \infty)$ yields

$$\int_{x_\mathrm{f}}^{\infty} \frac{d\Delta_\chi}{\Delta_\chi^2} \simeq -\int_{x_\mathrm{f}}^{\infty} dx \sum_n \lambda_n g_{\mathrm{eff}}^{1/2} x^{-n-2}. \tag{A4}$$

Evaluating the left-hand side gives

$$\frac{1}{\Delta_{\chi,\infty}} = \frac{1}{\Delta_{\chi,\mathrm{f}}} + \sum_n \int_{x_\mathrm{f}}^{\infty} dx \lambda_n g_{\mathrm{eff}}^{1/2} x^{-n-2}. \tag{A5}$$

Usually, the second term in the r.h.s. dominates.

It follows that the asymptotic anti-dark-matter abundance is

$$Y_{\chi,\infty} \simeq \Delta_{\chi,\infty} = \frac{1}{\sum_n \int_{x_\mathrm{f}}^{\infty} dx \lambda_n g_{\mathrm{eff}}^{1/2} x^{-n-2}}. \tag{A6}$$

Thus, substituting for λ_n and $g_{\mathrm{eff}}^{1/2}$,

$$Y_{\chi,\infty} \simeq \frac{1}{\sqrt{\frac{\pi}{45}} m_\chi M_{\mathrm{Pl}} g_*^{1/2} (1-r)^{-1/2} \sum_n \frac{\sigma_n x_\mathrm{f}^{-(n+3/2)}}{n+3/2} x_\star^{1/2}}, \tag{A7}$$

where we have observed that for our choice of parameters, $g_{\mathrm{eff}}^{1/2} \simeq (3/4) g_\star^{1/2} (1-r)^{-1/2} x^{-1/2} x_\star^{1/2}$. Therefore, including the dilution factor, the DM relic density is

$$\begin{aligned} \Omega_{\mathrm{DM}}^{\mathrm{Relic}} h^2 &= \zeta \frac{s_0 m_\chi}{\rho_c} h^2 Y_{\chi,\infty} \\ &\simeq \zeta \frac{1.0 \times 10^9 \ \mathrm{GeV}^{-1}}{M_{\mathrm{Pl}} g_\star^{1/2} (1-r)^{-1/2}} \left(\sum_n \frac{\sigma_n x_\mathrm{f}^{-(n+3/2)}}{n+3/2} x_\star^{1/2} \right)^{-1}, \end{aligned} \tag{A8}$$

where $\rho_c = 3H_0^2 M_{\mathrm{Pl}}^2/(8\pi)$, and $s_0 \simeq 2970 \ \mathrm{cm}^{-3}$.

1. Calculation for the freeze-out temperature

At freeze-out, the DM relic abundance stops tracking the equilibrium abundance; hence,

$$\Delta_\chi(x_\mathrm{f}) \simeq Y_{\chi,\mathrm{eq}}(x_\mathrm{f}) = \delta_\chi Y_{\chi,\mathrm{eq}}(x_\mathrm{f}), \tag{A9}$$

where δ_χ is a order of unity factor.

Neglecting $d\Delta_\chi/dx$ near freeze-out, from Eq. (A2), we may write

$$\left.\frac{dY_\chi}{dx}\right|_\mathrm{f} \approx -\sum_n \lambda_n \delta_\chi (\delta_\chi + 2) x_\mathrm{f}^{-n-2} g_{\mathrm{eff}}^{1/2}(x_\mathrm{f}) Y_{\chi,\mathrm{eq}}^2(x_\mathrm{f}). \tag{A10}$$

Also,

$$\frac{dY_{\chi,\mathrm{eq}}}{dx} = Y_{\chi,\mathrm{eq}} \left(\frac{3}{2x} - 1 \right); \tag{A11}$$

thus, using the approximation $dY_{\chi,\mathrm{eq}}/dx|_{\mathrm{FO}} \approx dY_{\chi}/dx|_{\mathrm{FO}}$, we obtain

$$\left(\frac{3}{2x_{\mathrm{f}}}-1\right) \approx -\left[\sum_n \delta_\chi(\delta_\chi+2)\lambda_n x_{\mathrm{f}}^{-n-2} g_{\mathrm{eff}}^{1/2}\right] Y_{\chi,\mathrm{eq}}(x_{\mathrm{f}}). \tag{A12}$$

Substituting for the equilibrium abundance $Y_{\chi,\mathrm{eq}}$ from Eq. (12) and using $(1-\frac{3}{2x_{\mathrm{f}}}) \approx 1$, we obtain

$$x_{\mathrm{f}} = \ln\left(b\left[\sum_n \delta_\chi(\delta_\chi+2)\lambda_n x_{\mathrm{f}}^{-n-1/2} g_{\mathrm{eff}}^{1/2}\right]\right). \tag{A13}$$

As argued by Scherrer and Turner [60], the numerical results suggest a best fit $(2\delta_\chi+\delta_\chi^2) \simeq n+1$. Substituting for g_{eff}, λ_n, and b, we obtain

$$\begin{aligned} x_{\mathrm{f}}^{\mathrm{MD}} &= \ln\left[\frac{\sqrt{45}g_\chi}{\sqrt{32}\pi^3} g_\star^{-1/2} \frac{M_{\mathrm{Pl}} m_\chi^{3/2}}{(1-r)^{1/2} T_\star^{1/2}} \sum_n \frac{(n+1)\sigma_n}{x_{\mathrm{f}}^{n+1}}\right], \\ x_{\mathrm{f}}^{\mathrm{RD}} &= \ln\left[\frac{\sqrt{45}g_\chi}{\sqrt{32}\pi^3} g_\star^{-1/2} M_{\mathrm{Pl}} m_\chi \sum_n \frac{(n+1)\sigma_n}{x_{\mathrm{f}}^{n+1/2}}\right]. \end{aligned} \tag{A14}$$

APPENDIX B: THERMALLY AVERAGED ANNIHILATION CROSS SECTION CALCULATION

1. Anapole moment

The differential cross section for the DM annihilation to the SM fermions (f) in the c.m. frame is given by

$$\left.\frac{d\sigma}{d\Omega}\right|_{\chi\bar{\chi}\to f\bar{f}} = \frac{1}{64\pi^2 s}\sqrt{\frac{s-4m_f^2}{s-4m_\chi^2}}|\bar{\mathcal{M}}_{f\bar{f}}|^2, \tag{B1}$$

where the spin-averaged squared amplitude reads

$$\begin{aligned} |\bar{\mathcal{M}}_{f\bar{f}}|^2 = \mathcal{C}_{\mathrm{AP}}^2 \frac{2e^2 g^2 C_F}{\Lambda^4}[&2m_\chi^4 - 4m_\chi^2(m_f^2+s+t) \\ &+ 2m_f^4 - 4m_f^2 t + s^2 + 2st + 2t^2], \end{aligned} \tag{B2}$$

in terms of Mandelstam variables s, t, and u and the SM fermion masses m_f. In the above, C_F denotes the color factor with a value $C_F = 3(1)$ for quarks (leptons), and the parameter $\mathcal{C}_{\mathrm{AP}}$ specifies whether the DM is a Dirac or Majorana fermion with the entry $\mathcal{C}_{\mathrm{AP}} = 1(1/2)$ for Dirac (Majorana) fermion.

In the NR limit, the thermally averaged annihilation cross section for the aforementioned process can be obtained as a power series expansion in the relative velocity of the incoming DM particles v_{rel}. At the leading order in v_{rel}, this can be expressed as

$$\begin{aligned} \langle\sigma v_{\mathrm{rel}}\rangle_{\chi\bar{\chi}\to f\bar{f}} = \mathcal{C}_{\mathrm{AP}}^2 \frac{2C_F \alpha g^2 m_\chi^2}{3\Lambda^4} \\ \times \sqrt{1-\frac{m_f^2}{m_\chi^2}}\left(1+\frac{m_f^2}{2m_\chi^2}\right)\langle v_{\mathrm{rel}}^2\rangle. \end{aligned} \tag{B3}$$

Similarly, the differential cross section for the DM annihilation to W^+W^- in the c.m. frame is given by

$$\left.\frac{d\sigma}{d\Omega}\right|_{\chi\bar{\chi}\to W^+W^-} = \frac{1}{64\pi^2 s}\sqrt{\frac{s-4m_W^2}{s-4m_\chi^2}}|\bar{\mathcal{M}}_{W^+W^-}|^2, \tag{B4}$$

$$\begin{aligned} |\bar{\mathcal{M}}_{W^+W^-}|^2 = -\frac{e^2 g^2}{2\Lambda^4 m_W^4}[&m_\chi^4(12m_W^4 - 4m_W^2 s + s^2) \\ &- 2m_\chi^2(12m_W^6 + 4m_W^4(7s+3t) \\ &- m_W^2 s(7s+4t) + s^2 t) + 12m_W^8 \\ &- 4m_W^6(s+6t) + m_W^4(17s^2+20st+12t^2) \\ &- 2m_W^2 s(2s^2+3st+2t^2) + s^2 t(s+t)]. \end{aligned} \tag{B5}$$

The thermally averaged annihilation cross section reads

$$\langle\sigma v_{\mathrm{rel}}\rangle_{\chi\bar{\chi}\to W^+W^-} = \frac{2\alpha g^2 m_\chi^6}{3\Lambda^4 m_W^4}\langle v_{\mathrm{rel}}^2\rangle. \tag{B6}$$

2. Electric dipole moment

If kinematically allowed, χ can annihilate into all the SM leptons and quarks as well as into the W boson and photons. The differential cross section for DM annihilation into SM fermions (f) in the c.m. frame is given by

$$\left.\frac{d\sigma}{d\Omega}\right|_{\chi\bar{\chi}\to f\bar{f}} = \frac{1}{64\pi^2 s}\sqrt{\frac{s-4m_f^2}{s-4m_\chi^2}}|\bar{\mathcal{M}}_{f\bar{f}}|^2, \tag{B7}$$

where the spin-averaged squared amplitude reads

$$\begin{aligned} |\bar{\mathcal{M}}_{f\bar{f}}|^2 = \frac{16C_F e^2 g^2}{\Lambda^2 s}[&2m_\chi^2 t + m_f^2(s+2t-2m_\chi^2) - m_\chi^4 \\ &- m_f^4 - t(s+t)], \end{aligned} \tag{B8}$$

in terms of the Mandelstam variables s, t, and u and the SM fermion masses m_f.

In the NR limit, the thermally averaged annihilation cross section can be expanded in the relative velocity v_{rel}. At leading order, one obtains

$$\langle\sigma v_{\mathrm{rel}}\rangle_{\chi\bar{\chi}\to f\bar{f}} = \frac{\alpha C_F g^2}{3\Lambda^2}\sqrt{1-\frac{m_f^2}{m_\chi^2}}\left(1+\frac{m_f^2}{2m_\chi^2}\right)\langle v_{\mathrm{rel}}^2\rangle. \tag{B9}$$

Similarly, the differential cross section for DM annihilation into W^+W^- in the c.m. frame is given by

$$\left.\frac{d\sigma}{d\Omega}\right|_{\chi\bar{\chi}\to W^+W^-} = \frac{1}{64\pi^2 s}\sqrt{\frac{s-4m_W^2}{s-4m_\chi^2}}|\bar{\mathcal{M}}_{W^+W^-}|^2, \quad \text{(B10)}$$

where

$$\begin{aligned}|\bar{\mathcal{M}}_{W^+W^-}|^2 = \frac{e^2g^2}{2\Lambda^2 m_W^4 s}[&4m_\chi^4(12m_W^4 - 4m_W^2 s + s^2)\\ &+ 4m_\chi^2(24m_W^6 + 12m_W^4(s-2t)\\ &- 2m_W^2 s(s-4t) - s^2(s+2t))\\ &+ 48m_W^8 - 32m_W^6(2s+3t)\\ &+ 16m_W^4 t(5s+3t) - 8m_W^2 st(3s+2t)\\ &+ s^2(s+2t)^2]. \end{aligned} \quad \text{(B11)}$$

In the NR limit, the corresponding thermally averaged annihilation cross section reads

$$\langle\sigma v_{\rm rel}\rangle_{\chi\bar{\chi}\to W^+W^-} = \frac{\alpha g^2 m_\chi^4}{3\Lambda^2 m_W^4}\langle v_{\rm rel}^2\rangle. \quad \text{(B12)}$$

DM can also annihilate into photons. The differential cross section is

$$\left.\frac{d\sigma}{d\Omega}\right|_{\chi\bar{\chi}\to\gamma\gamma} = \frac{1}{64\pi^2 s}\sqrt{\frac{s}{s-4m_\chi^2}}|\bar{\mathcal{M}}\gamma\gamma|^2 \quad \text{(B13)}$$

with

$$\begin{aligned}|\bar{\mathcal{M}}_{\gamma\gamma}|^2 = &\frac{64g^4}{\Lambda^4(m_\chi^2 - t)(m_\chi^2 - s - t)}\\ &\times [4m_\chi^6(s+t) - t^2(s+t)^2 + 4m_\chi^2 t(s+t)^2\\ &- m_\chi^4(s^2 + 10st + 6t^2) - m_\chi^8]. \end{aligned} \quad \text{(B14)}$$

In the nonrelativistic limit,

$$\langle\sigma v_{\rm rel}\rangle_{\chi\bar{\chi}\to\gamma\gamma} = \frac{g^4 m_\chi^2}{\pi\Lambda^4}(8 + 5\langle v_{\rm rel}^2\rangle). \quad \text{(B15)}$$

3. Magnetic dipole moment

Whenever kinematically accessible, χ can annihilate into all the SM leptons and quarks as well as into gauge boson final states such as W^+W^- and $\gamma\gamma$. The differential cross section for annihilation into SM fermions (f) in the c.m. frame is given by

$$\left.\frac{d\sigma}{d\Omega}\right|_{\chi\bar{\chi}\to f\bar{f}} = \frac{1}{64\pi^2 s}\sqrt{\frac{s-4m_f^2}{s-4m\chi^2}}|\bar{\mathcal{M}}_{f\bar{f}}|^2, \quad \text{(B16)}$$

where the corresponding spin-averaged squared amplitude takes the form

$$\begin{aligned}|\bar{\mathcal{M}}_{f\bar{f}}|^2 = \frac{16C_F e^2 g^2}{\Lambda^2 s}&[2m_\chi^2 t + 2m_\chi^2 s + m_f^2(s+2t+2m_\chi^2)\\ &- m_\chi^4 - m_f^4 - t(s+t)]. \end{aligned} \quad \text{(B17)}$$

Expanding in the relative velocity $v_{\rm rel}$, the thermally averaged annihilation cross section in the NR regime can be written as a velocity expansion. In the limit $m_f \to 0$, the leading contribution is

$$\langle\sigma v_{\rm rel}\rangle_{\chi\bar{\chi}\to f\bar{f}} = \frac{4\alpha C_F g^2}{\Lambda^2}\left(1 - \frac{1}{24}\langle v_{\rm rel}^2\rangle\right). \quad \text{(B18)}$$

For annihilation into W^+W^-, the differential cross section in the c.m. frame is given by

$$\left.\frac{d\sigma}{d\Omega}\right|_{\chi\bar{\chi}\to W^+W^-} = \frac{1}{64\pi^2 s}\sqrt{\frac{s-4m_W^2}{s-4m\chi^2}}|\bar{\mathcal{M}}_{W^+W^-}|^2 \quad \text{(B19)}$$

with the squared amplitude

$$\begin{aligned}|\bar{\mathcal{M}}_{W^+W^-}|^2 = \frac{e^2g^2}{2\Lambda^2 m_W^4 s}&[4m_\chi^4(12m_W^4 - 4m_W^2 s + s^2)\\ &- 8m_\chi^2(12m_W^6 + 4m_W^4(7s+3t)\\ &- m_W^2 s(7s+4t) + s^2 t) + 48m_W^8\\ &- 32m_W^6(2s+3t) + 16m_W^4 t(5s+3t)\\ &- 8m_W^2 st(3s+2t) + s^2(s+2t)^2]. \end{aligned} \quad \text{(B20)}$$

The associated thermally averaged cross section in the NR limit is given by

$$\langle\sigma v_{\rm rel}\rangle_{\chi\bar{\chi}\to W^+W^-} = \frac{4\alpha g^2 m_\chi^4}{\Lambda^2 m_W^4}\left(1 + \frac{\langle v_{\rm rel}^2\rangle}{3}\right). \quad \text{(B21)}$$

In addition, annihilation into photons proceeds via t- and u-channel contributions. The corresponding differential cross section is

$$\left.\frac{d\sigma}{d\Omega}\right|_{\chi\bar{\chi}\to\gamma\gamma} = \frac{1}{64\pi^2 s}\sqrt{\frac{s}{s-4m\chi^2}}|\bar{\mathcal{M}}_{\gamma\gamma}|^2, \quad \text{(B22)}$$

where the squared matrix element is

$$\begin{aligned}|\bar{\mathcal{M}}_{\gamma\gamma}|^2 = &\frac{64g^4}{\Lambda^4(m_\chi^2 - t)(m_\chi^2 - s - t)}\\ &\times [4m_\chi^6(s+t) - t^2(s+t)^2 + 4m_\chi^2 t(s+t)^2\\ &- m_\chi^4(s^2 + 10st + 6t^2) - m_\chi^8]. \end{aligned} \quad \text{(B23)}$$

In the NR limit, the thermally averaged annihilation cross section takes the form

$$\langle \sigma v_{\rm rel} \rangle_{\chi\bar{\chi}\to\gamma\gamma} = \frac{g^4 m_\chi^2}{\pi\Lambda^4}(8 + 5\langle v_{\rm rel}^2 \rangle). \tag{B24}$$

4. Charge radius

χ can annihilate into all the SM leptons and quarks. The spin-averaged squared amplitude is given by

$$|\bar{\mathcal{M}}_{f\bar{f}}|^2 = \frac{2e^2 g^2 C_F}{\Lambda^4}[2m_\chi^4 + 4m_\chi^2(m_f^2 - t) + 2m_f^4 - 4m_f^2 t + s^2 + 2st + 2t^2]. \tag{B25}$$

In the NR regime, the thermally averaged annihilation cross section can be expanded in powers of the relative velocity $v_{\rm rel}$. In the limit $m_f \to 0$, the leading contribution takes the form

$$\langle \sigma v_{\rm rel} \rangle_{\chi\bar{\chi}\to f\bar{f}} = \frac{\alpha g^2 C_F m_\chi^2}{\Lambda^4}\left(4 + \frac{7}{6}\langle v_{\rm rel}^2 \rangle\right). \tag{B26}$$

For annihilation into W^+W^-, the differential cross section in the c.m. frame is given by

$$\left.\frac{d\sigma}{d\Omega}\right|_{\chi\bar{\chi}\to W^+W^-} = \frac{1}{64\pi^2 s}\sqrt{\frac{s - 4m_W^2}{s - 4m\chi^2}}|\bar{\mathcal{M}}_{W^+W^-}|^2, \tag{B27}$$

with the squared amplitude

$$\begin{aligned}\overline{|\mathcal{M}}_{W^+W^-}|^2 = -\frac{e^2 g^2}{2\Lambda^4 m_W^4}[&m_\chi^4(12m_W^4 - 4m_W^2 s + s^2) \\ &- 2m_\chi^2(12m_W^6 + 4m_W^4(7s + 3t) \\ &- m_W^2 s(7s + 4t) + s^2 t) + 12m_W^8 \\ &- 4m_W^6(s + 6t) + m_W^4(17s^2 + 20st + 12t^2) \\ &- 2m_W^2 s(2s^2 + 3st + 2t^2) + s^2 t(s + t)].\end{aligned} \tag{B28}$$

The thermally averaged cross section in the NR limit is given by

$$\langle \sigma v_{\rm rel} \rangle_{\chi\bar{\chi}\to W^+W^-} = \frac{\alpha g^2 m_\chi^6}{\Lambda^4 m_W^4}\left(4 + \frac{19}{6}\langle v_{\rm rel}^2 \rangle\right). \tag{B29}$$

[1] R. Allahverdi *et al.*, The first three seconds: A review of possible expansion histories of the early universe, Open J. Astrophys. **4**, astro.2006.16182 (2021).
[2] M. Kamionkowski and M. S. Turner, Thermal relics: Do we know their abundances?, Phys. Rev. D **42**, 3310 (1990).
[3] G. F. Giudice, E. W. Kolb, and A. Riotto, Largest temperature of the radiation era and its cosmological implications, Phys. Rev. D **64**, 023508 (2001).
[4] T. Moroi and L. Randall, Wino cold dark matter from anomaly mediated SUSY breaking, Nucl. Phys. **B570**, 455 (2000).
[5] D. H. Lyth, Dilution of cosmological densities by saxino decay, Phys. Rev. D **48**, 4523 (1993).
[6] G. Gelmini, P. Gondolo, A. Soldatenko, and C. E. Yaguna, The Effect of a late decaying scalar on the neutralino relic density, Phys. Rev. D **74**, 083514 (2006).
[7] G. B. Gelmini and P. Gondolo, Neutralino with the right cold dark matter abundance in (almost) any supersymmetric model, Phys. Rev. D **74**, 023510 (2006).
[8] B. S. Acharya, G. Kane, S. Watson, and P. Kumar, A non-thermal WIMP miracle, Phys. Rev. D **80**, 083529 (2009).
[9] G. L. Kane, P. Kumar, B. D. Nelson, and B. Zheng, Dark matter production mechanisms with a nonthermal cosmological history: A classification, Phys. Rev. D **93**, 063527 (2016).
[10] H. Davoudiasl, D. Hooper, and S. D. McDermott, Inflatable dark matter, Phys. Rev. Lett. **116**, 031303 (2016).
[11] L. Randall, J. Scholtz, and J. Unwin, Flooded dark matter and S level rise, J. High Energy Phys. 03 (2016) 011.
[12] R. T. Co, F. D'Eramo, L. J. Hall, and D. Pappadopulo, Freeze-in dark matter with displaced signatures at colliders, J. Cosmol. Astropart. Phys. 12 (2015) 024.
[13] J. A. Dror, E. Kuflik, and W. H. Ng, Codecaying dark matter, Phys. Rev. Lett. **117**, 211801 (2016).
[14] A. Banerjee and D. Chowdhury, Fingerprints of freeze-in dark matter in an early matter-dominated era, SciPost Phys. **13**, 022 (2022).
[15] M. Y. Khlopov and A. G. Polnarev, Primordial black holes as a cosmological test of grand unification, Phys. Lett. **97B**, 383 (1980).
[16] S. Datta, A. Ghoshal, A. Spalding, and G. White, Gravitational wave spectral shapes as a probe of long lived right-handed neutrinos, leptogenesis and dark matter. Global versus local B–L cosmic strings, J. High Energy Phys. 03 (2026) 245.
[17] H. Mansour, Y. Gouttenoire, and F. Kahlhoefer, Can the universe be matter-dominated after a supercooled first-order phase transition?, arXiv:2607.19469.
[18] E. W. Kolb and M. S. Turner, *The Early Universe*, Vol. 69 (Taylor and Francis, London, 2019).
[19] S. Hamdan and J. Unwin, Dark matter freeze-out during matter domination, Mod. Phys. Lett. A **33**, 1850181 (2018).
[20] P. Chanda, S. Hamdan, and J. Unwin, Reviving Z and Higgs mediated dark matter models in matter dominated freeze-out, J. Cosmol. Astropart. Phys. 01 (2020) 034.

[21] P. Chanda and J. Unwin, Decoupling of asymmetric dark matter during an early matter dominated era, J. Cosmol. Astropart. Phys. 06 (2021) 032.
[22] P. Asadi, T. R. Slatyer, and J. Smirnov, WIMPs without weakness: Generalized mass window with entropy injection, Phys. Rev. D **106**, 015012 (2022).
[23] G. Steigman and M. S. Turner, Cosmological constraints on the properties of weakly interacting massive particles, Nucl. Phys. **B253**, 375 (1985).
[24] G. Jungman, M. Kamionkowski, and K. Griest, Supersymmetric dark matter, Phys. Rep. **267**, 195 (1996).
[25] G. Bertone, D. Hooper, and J. Silk, Particle dark matter: Evidence, candidates and constraints, Phys. Rep. **405**, 279 (2005).
[26] G. Steigman, B. Dasgupta, and J. F. Beacom, Precise relic WIMP abundance and its impact on searches for dark matter annihilation, Phys. Rev. D **86**, 023506 (2012).
[27] G. Arcadi, M. Dutra, P. Ghosh, M. Lindner, Y. Mambrini, M. Pierre, S. Profumo, and F. S. Queiroz, The waning of the WIMP? A review of models, searches, and constraints, Eur. Phys. J. C **78**, 203 (2018).
[28] A. Kundu, S. Maharana, and P. Mondal, A 96 GeV scalar tagged to dark matter models, Nucl. Phys. **B955**, 115057 (2020).
[29] W. L. Xu, C. Dvorkin, and A. Chael, Probing sub-GeV dark matter-baryon scattering with cosmological observables, Phys. Rev. D **97**, 103530 (2018).
[30] C. Dvorkin, T. Lin, and K. Schutz, Making dark matter out of light: Freeze-in from plasma effects, Phys. Rev. D **99**, 115009 (2019); **105**, 119901(E) (2022).
[31] J. H. Chang, R. Essig, and S. D. McDermott, Supernova 1987A constraints on sub-GeV dark sectors, millicharged particles, the QCD axion, and an axion-like particle, J. High Energy Phys. 09 (2018) 051.
[32] A. Caputo, L. Sberna, M. Frias, D. Blas, P. Pani, L. Shao, and W. Yan, Constraints on millicharged dark matter and axionlike particles from timing of radio waves, Phys. Rev. D **100**, 063515 (2019).
[33] D. F. G. Fiorillo and E. Vitagliano, Self-interacting dark sectors in supernovae can behave as a relativistic fluid, Phys. Rev. Lett. **133**, 251004 (2024).
[34] E. Iles, S. Heeba, and K. Schutz, Dark matter direct detection experiments are sensitive to the millicharged background, Phys. Rev. Lett. **134**, 121002 (2025).
[35] I. B. Zel'dovich, Electromagnetic interaction with parity violation, Sov. Phys. JETP **6**, 1184 (1958), https://www.jetp.ras.ru/cgi-bin/dn/e_006_06_1184.pdf.
[36] M. Pospelov and T. ter Veldhuis, Direct and indirect limits on the electromagnetic form-factors of WIMPs, Phys. Lett. B **480**, 181 (2000).
[37] K. Sigurdson, M. Doran, A. Kurylov, R. R. Caldwell, and M. Kamionkowski, Dark-matter electric and magnetic dipole moments, Phys. Rev. D **70**, 083501 (2004); **73**, 089903 (E) (2006).
[38] E. Masso, S. Mohanty, and S. Rao, Dipolar dark matter, Phys. Rev. D **80**, 036009 (2009).
[39] V. Barger, W.-Y. Keung, and D. Marfatia, Electromagnetic properties of dark matter: Dipole moments and charge form factor, Phys. Lett. B **696**, 74 (2011).
[40] C. M. Ho and R. J. Scherrer, Anapole dark matter, Phys. Lett. B **722**, 341 (2013).
[41] B. J. Kavanagh, P. Panci, and R. Ziegler, Faint light from dark matter: Classifying and constraining dark matter-photon effective operators, J. High Energy Phys. 04 (2019) 089.
[42] T. Hambye and X.-J. Xu, Dark matter electromagnetic dipoles: The WIMP expectation, J. High Energy Phys. 11 (2021) 156.
[43] A. Ibarra, M. Reichard, and R. Nagai, Anapole moment of Majorana fermions and implications for direct detection of neutralino dark matter, J. High Energy Phys. 01 (2022) 086.
[44] E. E. Radescu, On the electromagnetic properties of majorana fermions, Phys. Rev. D **32**, 1266 (1985).
[45] T. Banks, J.-F. Fortin, and S. Thomas, Direct detection of dark matter electromagnetic dipole moments, arXiv:1007.5515.
[46] E. Del Nobile, G. B. Gelmini, P. Gondolo, and J.-H. Huh, Direct detection of light anapole and magnetic dipole DM, J. Cosmol. Astropart. Phys. 06 (2014) 002.
[47] S. Chatterjee and R. Laha, Explorations of pseudo-Dirac dark matter having keV splittings and interacting via transition electric and magnetic dipole moments, Phys. Rev. D **107**, 083036 (2023).
[48] D. Bose, D. Chowdhury, P. Mondal, and T. S. Ray, Troubles mounting for multipolar dark matter, J. High Energy Phys. 06 (2023) 014.
[49] A. Ibarra, M. Reichard, and G. Tomar, Probing dark matter electromagnetic properties in direct detection experiments, J. Cosmol. Astropart. Phys. 02 (2024) 072.
[50] J. Kumar, B. Mondal, G. Muralidhara, and N. Raj, Direct detection of electromagnetically interacting ultraheavy dark matter, J. High Energy Phys. 07 (2026) 082.
[51] B. Geytenbeek, S. Rao, P. Scott, A. Serenelli, A. C. Vincent, M. White, and A. G. Williams, Effect of electromagnetic dipole dark matter on energy transport in the solar interior, J. Cosmol. Astropart. Phys. 03 (2016) 029.
[52] G. Lambiase, S. Mohanty, A. Nautiyal, and S. Rao, Constraints on electromagnetic form factors of sub-GeV dark matter from the cosmic microwave background anisotropy, Phys. Rev. D **104**, 023519 (2021).
[53] S. Das, R. Mondol, A. Singh, and R. Laha, Dark secrets of baryons: Illuminating dark matter-baryon interactions with JWST, Phys. Rev. Lett. **137**, 011002 (2026).
[54] J.-F. Fortin and T. M. P. Tait, Collider Constraints on dipole-interacting dark matter, Phys. Rev. D **85**, 063506 (2012).
[55] X. Chu, J. Pradler, and L. Semmelrock, Light dark states with electromagnetic form factors, Phys. Rev. D **99**, 015040 (2019).
[56] D. Biswas, Study of sub-GeV dipolar dark states at SND@LHC within invisible bounds on meson decays, Eur. Phys. J. C **86**, 815 (2026).
[57] R. J. Scherrer and M. S. Turner, Decaying particles do not "heat up" the Universe, Phys. Rev. D **31**, 681 (1985).
[58] B. Spokoiny, Deflationary universe scenario, Phys. Lett. B **315**, 40 (1993).
[59] M. L. Graesser, I. M. Shoemaker, and L. Vecchi, Asymmetric WIMP dark matter, J. High Energy Phys. 10 (2011) 110.

[60] R. J. Scherrer and M. S. Turner, On the relic, cosmic abundance of stable weakly interacting massive particles, Phys. Rev. D **33**, 1585 (1986); **34**, 3263(E) (1986).
[61] T. Hasegawa, N. Hiroshima, K. Kohri, R. S. L. Hansen, T. Tram, and S. Hannestad, MeV-scale reheating temperature and thermalization of oscillating neutrinos by radiative and hadronic decays of massive particles, J. Cosmol. Astropart. Phys. 12 (2019) 012.
[62] E. Del Nobile, The theory of direct dark matter detection: A guide to computations, Lect. Notes Phys. 996 (2022).
[63] Y. Gao, C. M. Ho, and R. J. Scherrer, Anapole dark matter at the LHC, Phys. Rev. D **89**, 045006 (2014).
[64] C. Arina, A. Cheek, K. Mimasu, and L. Pagani, Light and darkness: Consistently coupling dark matter to photons via effective operators, Eur. Phys. J. C **81**, 223 (2021).
[65] S. Y. Choi, J. Jeong, D. W. Kang, and S. Shin, Hunting for hypercharge anapole dark matter in all spin scenarios, Phys. Rev. D **109**, 096001 (2024).
[66] PandaX Collaboration, Limits on the luminance of dark matter from xenon recoil data, Nature (London) **618**, 47 (2023).
[67] J.-H. Liang, Y. Liao, X.-D. Ma, and H.-L. Wang, A systematic investigation on dark matter-electron scattering in effective field theories, J. High Energy Phys. 07 (2024) 279.
[68] I. Jeong, S. Kang, S. Scopel, and G. Tomar, WimPyDD: An object–oriented Python code for the calculation of WIMP direct detection signals, Comput. Phys. Commun. **276**, 108342 (2022).
[69] M. G. Aartsen *et al.* (IceCube Collaboration), Search for annihilating dark matter in the Sun with 3 years of IceCube data, Eur. Phys. J. C **77**, 146 (2017); **79**, 214(E) (2019).
[70] R. K. Leane, K. C. Y. Ng, and J. F. Beacom, Powerful solar signatures of long-lived dark mediators, Phys. Rev. D **95**, 123016 (2017).
[71] D. Bose, T. N. Maity, and T. S. Ray, Neutrinos from captured dark matter annihilation in a galactic population of neutron stars, J. Cosmol. Astropart. Phys. 05 (2022) 001.
[72] R. Abbasi *et al.* (IceCube Collaboration), Search for GeV-scale dark matter annihilation in the Sun with IceCube DeepCore, Phys. Rev. D **105**, 062004 (2022).
[73] T. N. Maity, A. K. Saha, S. Mondal, and R. Laha, Neutrinos from the Sun can discover dark matter-electron scattering, Phys. Rev. D **112**, 023025 (2025).
[74] D. Bose, R. Pramanick, and T. S. Ray, Neutrinos from captured dark matter in galactic stars, Phys. Lett. B **866**, 139542 (2025).
[75] D. Krishna, R. Sherpa, A. K. Saha, T. N. Maity, R. Laha, and N. Raj, ν limits from super-Kamiokande on dark matter-electron scattering in the Sun, arXiv:2503.07713.
[76] R. Abbasi *et al.* (IceCube Collaboration), Search for high-energy neutrinos from the sun using ten years of IceCube data, arXiv:2507.08457.
[77] T. T. Q. Nguyen, T. Linden, P. Carenza, and A. Widmark, Super-Kamiokande strongly constrains leptophilic dark matter capture in the Sun, Phys. Rev. D **113**, L101305 (2026).
[78] T. T. Q. Nguyen and T. Linden, The Sun can strongly constrain spin-dependent dark matter nucleon scattering below the evaporation limit, arXiv:2602.15113.
[79] T. T. Q. Nguyen, Constraints and projections for milli-charged dark matter in the Sun with water cherenkov neutrino detectors, arXiv:2606.09998.
[80] R. Garani and S. Palomares-Ruiz, Dark matter in the Sun: Scattering off electrons vs nucleons, J. Cosmol. Astropart. Phys. 05 (2017) 007.
[81] G. Busoni, A. De Simone, P. Scott, and A. C. Vincent, Evaporation and scattering of momentum- and velocity-dependent dark matter in the Sun, J. Cosmol. Astropart. Phys. 10 (2017) 037.
[82] D. Bose and S. Sarkar, Impact of galactic distributions in celestial capture of dark matter, Phys. Rev. D **107**, 063010 (2023).
[83] N. Vinyoles, A. M. Serenelli, F. L. Villante, S. Basu, J. Bergström, M. C. Gonzalez-Garcia, M. Maltoni, C. Peña-Garay, and N. Songg, A new generation of standard solar models, Astrophys. J. **835**, 202 (2017).
[84] R. H. Helm, Inelastic and elastic scattering of 187-Mev electrons from selected even-even nuclei, Phys. Rev. **104**, 1466 (1956).
[85] Z.-L. Liang, Y.-L. Tang, and Z.-Q. Yang, The leptophilic dark matter in the Sun: The minimum testable mass, J. Cosmol. Astropart. Phys. 10 (2018) 035.
[86] R. Garani and S. Palomares-Ruiz, Evaporation of dark matter from celestial bodies, J. Cosmol. Astropart. Phys. 05 (2022) 042.
[87] Q. Liu, J. Lazar, C. A. Argüelles, and A. Kheirandish, χAROν: A tool for neutrino flux generation from WIMPs, J. Cosmol. Astropart. Phys. 10 (2020) 043.
[88] C. A. Argüelles, J. Salvado, and C. N. Weaver, nuSQuIDS: A toolbox for neutrino propagation, Comput. Phys. Commun. **277**, 108346 (2022).
[89] N. Aghanim *et al.* (Planck Collaboration), Planck 2018 results. VI. Cosmological parameters, Astron. Astrophys. **641**, A6 (2020); **652**, C4(E) (2021).
[90] N. Anand, A. L. Fitzpatrick, and W. C. Haxton, Weakly interacting massive particle-nucleus elastic scattering response, Phys. Rev. C **89**, 065501 (2014).
[91] C. Pallis, Massive particle decay and cold dark matter abundance, Astropart. Phys. **21**, 689 (2004).
[92] A. Ibarra, M. Reichard, and G. Tomar, Celestial probes of dark matter electromagnetic interactions, arXiv:2608.27957.
[93] J. C. Criado, A. Djouadi, M. Perez-Victoria, and J. Santiago, A complete effective field theory for dark matter, J. High Energy Phys. 07 (2021) 081.
[94] S. Jahedi, Neutron stars as thermometers for reheating induced dipole dark matter, arXiv:2607.01390.